

FHL2 switches MITF from activator to repressor of Erbin expression during cardiac hypertrophy



Inbal Rachmin^{a,1,2,3,4}, Eden Amsalem^{a,2}, Eliahu Golomb^{b,3}, Ronen Beeri^c, Dan Gilon^{c,3}, Pengfei Fang^{d,2}, Hovav Nechushtan^{e,3}, Gillian Kay^{a,4}, Min Guo^{d,2,3}, Peter Li Yiqing^{f,2,3}, Roger S.-Y. Foo^{f,*,2}, David E. Fisher^{g,*,3}, Ehud Razin^{a,*,1}, Sagi Tshori^{h,1}

^a Department of Biochemistry and Molecular Biology, The Institute for Medical Research Israel–Canada, Hebrew University Medical School, Jerusalem 91120, Israel

^b Department of Pathology, Shaare Zedek Medical Center, Jerusalem 91031, Israel

^c Heart Institute, Hadassah-Hebrew University Medical Center, P.O. Box 12000, Jerusalem 91120, Israel

^d Department of Cancer Biology, The Scripps Research Institute, 130 Scripps Way, Jupiter, FL 33458, USA

^e Sharett Institute of Oncology, Hadassah Hebrew University Medical center, P.O. Box 12000, Jerusalem 91120, Israel

^f Cardiovascular Research institute, Center of Translational Medicine, National University of Singapore, 117599, Singapore

^g Cutaneous Biology Research Center, Department of Dermatology, Massachusetts General Hospital, Harvard Medical School, Building 149, 13th Street Charlestown, Boston, MA 02129, USA

^h Department of Nuclear Medicine, Hadassah-Hebrew University Medical Center, P.O. Box 12000, Jerusalem 91120, Israel

ARTICLE INFO

Article history:

Received 20 January 2015

Received in revised form 26 April 2015

Accepted 6 May 2015

Available online 20 May 2015

Keywords:

MITF
FHL2
Erbin
Activator
Repressor
Gene regulation

ABSTRACT

Background: Congestive heart failure (CHF) is a significant health care burden in developed countries. However, the molecular events leading from cardiac hypertrophy to CHF are unclear and preventive therapeutic approaches are limited. We have previously described that microphthalmia-associated transcription factor (MITF) is a key regulator of cardiac hypertrophy, but its cardiac targets are still uncharacterized.

Methods and results: Gene array analysis of hearts from MITF-mutated mice indicated that Erbb2 interacting protein (Erbin) is a candidate target gene for MITF. We have recently demonstrated that Erbin is decreased in human heart failure and plays a role as a negative modulator of pathological cardiac hypertrophy. Here we show that Erbin expression is regulated by MITF. Under basal conditions MITF activates Erbin expression by direct binding to its promoter. However, under β -adrenergic stimulation Erbin expression is decreased only in wild type mice, but not in MITF-mutated mice. Yeast two-hybrid screening, using MITF as bait, identified an interaction with the cardiac-predominant four-and-a-half LIM domain protein 2 (FHL2), which was confirmed by co-immunoprecipitation in both mouse and human hearts. Upon β -adrenergic stimulation, FHL2 and MITF bind Erbin promoter as a complex and repress MITF-directed Erbin expression. Overexpression of FHL2 alone had no effect on Erbin expression, but in the presence of MITF, Erbin expression was decreased. FHL2–MITF association was also increased in biopsies of heart failure patients.

Conclusion: MITF unexpectedly regulates both the activation and the repression of Erbin expression. This ligand mediated fine tuning of its gene expression could be an important mechanism in the process of cardiac hypertrophy and heart failure.

© 2015 Elsevier Ireland Ltd. All rights reserved.

1. Introduction

MITF is a basic helix–loop–helix leucine zipper (bHLH-Zip) DNA-binding protein [1]. Its gene resides at the *mi* locus in mice [2]. Mutations of this gene result in deafness, small eyes, and poorly pigmented eyes and skin [3]. In humans, heterozygous mutations in this gene cause

Waardenburg Syndrome type II [4], resulting in hypopigmentation and deafness.

MITF regulates gene transcription by binding to E-box elements in the 5′-flanking regions or functional enhancers of MITF-responsive genes [5]. MITF functions as either a homodimer or heterodimer with transcription factors of the related MiT family [5,6].

We have previously demonstrated that the H isoform of MITF is highly expressed in cardiomyocytes [7], and that MITF-mutated mice have a diminished cardiac hypertrophic response to β -adrenergic stimulation, decreased cardiac function and a tendency for sudden death [8]. Moreover, we reported that middle-aged MITF-mutated mice have a much smaller heart mass and decreased cardiac function and output [8]. These observations indicate that MITF plays an essential role in the

* Corresponding authors.

E-mail addresses: mdcrfsy@nus.edu.sg (R.S.-Y. Foo), ehudr@ekmd.huji.ac.il (E. Razin).

¹ This author takes responsibility for all aspects of the reliability and freedom from bias of the data presented and their discussed interpretation.

² This author performed the experiments.

³ This author analyzed the data.

⁴ This author wrote the paper.

development of cardiac hypertrophy [8]. In order to identify cardiac MITF target genes, we conducted a gene array analysis of mRNA from a pool of hearts derived from middle-aged MITF mutated mice (*ce/ce*) and compared it to that from their normal siblings (*sp/sp*).

One of the candidate target genes identified in this assay was the ErbB2 interacting protein (Erbin). Erbin is a member of the leucine-rich repeat and PDZ domain (LAP) proteins [9]. It was originally described as a binding partner of Her2/neu (ErbB2) [9]. We recently reported that Erbin is involved in cardiac hypertrophy. When cardiac hypertrophy was induced, *Erbin*^{-/-} mice developed heart failure and following severe pressure overload all *Erbin*^{-/-} mice died [10]. Little was known regarding the regulation of Erbin expression. The transcription factor c-Myb has been shown to directly regulate Erbin in HeLa cells [11], but no transcription factor regulating Erbin expression in the heart has been reported.

Here we used *in silico*, *in vitro* and *in vivo* approaches to demonstrate that Erbin expression in the heart is directly regulated by MITF. Under basal conditions MITF activates Erbin expression by binding two E-box elements in the Erbin promoter, whereas following β -adrenergic stimulation, MITF inhibits Erbin expression. We further found that this inhibition by MITF is mediated by its interaction with Four and a half LIM domain protein 2 (FHL2) while MITF is bound to its target gene. FHL2 is a LIM domain binding protein expressed predominately in the heart and in smooth muscle cells [12]. FHL2–MITF interaction is mediated by the LIM2 and LIM3 domains of FHL2 and the bHLH domain of MITF. Thus, activation/repression of Erbin expression in the heart is regulated by FHL2–MITF interaction.

2. Material and methods

2.1. Cell culture

HEK293T, NIH3T3 and H9c2 cells were maintained at 37 °C in growth medium, which was Dulbecco's modified Eagle's medium (DMEM; Sigma-Aldrich) supplemented with 4 mM L-glutamine, 100 units/ml penicillin, 100 μ g/ml streptomycin and 10% fetal bovine serum (Biological Industries). Cells were serum-starved for 18 h in DMEM and treated with 10 μ M isoproterenol (Sigma-Aldrich) overnight. Myocardial cells from ventricle fragments of hearts of 1 day old Sprague–Dawley rats were isolated by serial trypsinization as previously described [13]. Cells were suspended in F-10 medium containing 10% heat-inactivated FBS and 10% horse serum and penicillin–streptomycin antibiotic solution (Biological Industries). This medium was also used as the standard culture medium in the experiments. The cell suspensions were enriched for cardiomyocytes by pre-plating on tissue culture dishes for 30 min to allow attachment of fibroblasts. The cells were plated on 60 mm Petri dishes at a density of 10⁶ cells/ml. For isoproterenol treatment cells were incubated with serum-free medium for 18 h and treated with 10 μ M of isoproterenol (Sigma-Aldrich) for an additional 18 h.

2.2. Human left ventricular biopsies

Human left ventricular tissue was collected following a protocol approved by the Papworth (Cambridge) Hospital Tissue Bank Review Board and the Cambridgeshire Research Ethics Committee (United Kingdom). Written consent was obtained from every individual according to the Papworth Tissue Bank protocol. Left ventricular (LV) tissue was obtained from non-donor suitable healthy male individuals involved in road traffic accidents. At the time of transplantation or donor harvest, whole hearts were removed after preservation and transported in cold cardioplegic solution (cardioplegia formula and Hartmann's solution) similar to the procedure described before at Imperial College, London [14]. Following analysis by a cardiovascular pathologist, left ventricular segments were cut and stored immediately in RNAlater (Ambion).

2.3. Mice

All mouse lines were held and propagated in a specific pathogen-free environment. Both MITF *sp/sp* and MITF *sp/ce* mice were kindly provided by L. Lamoreux (College of Veterinary Medicine, Texas A&M University, and College Station, Texas, USA), were on a C57BL/6 background and were bred to produce *sp/sp* and *ce/ce* mice for experiments. MITF encoded by the mutated mouse allele (*ce/ce*) lacks the zip domain of MITF due to a stop codon between the HLH and zip domains while their normal littermates (*sp/sp*) express the full-length protein, apart from the six amino acids of exon 6a [15]. VEGA-9tg/+ mice were kindly provided by H. Arnheiter (NIH, Bethesda, Maryland, USA). Mice carrying the *tg/tg* mutation have an insertion of approximately 50 copies of a transgene integrated inside the MITF promoter and are unable to express MITF. Mice aged 6–8 weeks were used for all the experiments apart from those represented in Fig. 1, for which 15 month old mice were used.

All experiments were performed in compliance with the Israeli Prevention of Cruelty to Animals Law and were approved by the Hebrew University Animal Care and Use Committee.

2.4. Administration of isoproterenol

For the induction of cardiac hypertrophy, 6 week old *sp/sp* and *ce/ce* MITF mutant mice were administered either 5 mg/kg isoproterenol (Sigma-Aldrich) or saline subcutaneously to the neck once a day for 7 days.

For the co-immunoprecipitation assay, 8 week old wild type (WT) mice were administered either 15 mg/kg isoproterenol (Sigma-Aldrich) or saline intraperitoneally (i.p) once a day for 5 days.

2.5. Gene array

Gene array membranes covering the known coding sequences of the entire mouse genome were printed using MicroGrid II Compact (BioRobotics) by the Interdepartmental Unit of the Medical School of the Hebrew University and Hadassah Medical Center. RNA was extracted from a pool of 15 month old normal (*sp/sp*) and *ce/ce* MITF mutated mice. The RNA was reversed transcribed, tagged by Cy3 and Cy5, and hybridized to the mouse custom-made mRNA array. Results were read using the GenePix 4000B system (Molecular Devices) and analyzed using Matlab written processing routines.

2.6. Antibodies

Anti-Erbin antibody (rabbit polyclonal sera) was kindly provided by Prof. Jean Borg (Marseille, France) and anti-MITF antibody (C5-mouse monoclonal) was kindly provided by Prof. David E. Fisher (Dana-Farber Cancer Institute and Children's Hospital, Boston, MA). Anti- β -actin antibody (Sigma-Aldrich), anti-tubulin antibody, anti-GAPDH (Santa Cruz) and anti-FHL2 (MBL) were purchased. These antibodies were used for EMSA, ChIP and Western blots.

2.7. Real-time quantitative PCR

Candidate MITF and Erbin responsive genes were measured using real-time quantitative PCR. Total RNA was extracted from the hearts of *ce/ce*, *sp/sp* and WT mice. mRNA levels of various genes were quantified by SYBR Green incorporation (ABgene SYBR green ROX Mix, ABgene). Real-time PCR was performed on the Rotor-Gene 3000 sequence detection system (Corbett).

The primers used for gene amplification for real-time PCR were as follows: β -actin sense, 5'-CCTGATCCACATCTGCTGAA-3'; β -actin antisense, 5'-ATTGCCGACAGGATGCAGA A-3'; Erbin sense, 5'-GCATCCGCAGACATCCAGTCCA-3'; Erbin antisense, 5'-GGCTGGC CCATTTGTCCATTA

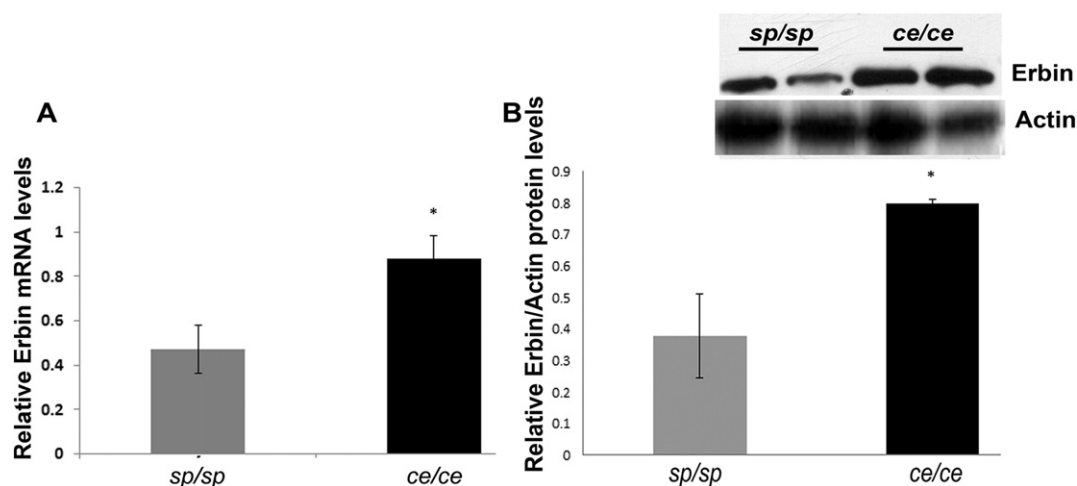


Fig. 1. Erbin expression in the heart of 15 month old MITF mutated mice (*ce/ce*) compared to wild type littermates (*sp/sp*). A. Real-time PCR analysis of Erbin expression in hearts from *ce/ce* ($n = 7$) and *sp/sp* mice ($n = 9$). Results were normalized to β actin. Results represent mean \pm SEM. B. Western blot analysis of Erbin and β actin (control) protein levels in hearts from *ce/ce* ($n = 4$) and *sp/sp* mice ($n = 4$) using anti-Erbin and anti- β actin antibodies. Each lane represents one mouse. Bar graph represents the densitometry quantification of Western data, normalized to β actin. Results represent mean \pm SEM.

CT-3'; and FHL2 sense, 5' TCACAGCACGGGATGAGTTTC 3'; FHL2 anti-sense, 5' GTGCCACCCAGACCACTAATG 3'.

2.8. Plasmid construction

FHL2-CMV5 vector was kindly provided by Prof. Paul Riley (Oxford University). MITF-H was amplified by PCR and then excised and ligated into pCMV-Tag 4A vector (Agilent Technologies) using XbaI and HindIII (New England Biolabs, Inc.). The Erbin promoter was amplified using PCR of genomic mouse DNA, and the fragment from -1500 to -3000 was excised using KpnI and NheI (New England Biolabs, Inc.) and ligated into a pGL3 vector (Promega) containing a luciferase reporter gene. Mutations of Erbin promoter were generated using the QuickChange mutagenesis SDM kit (Agilent Technologies) with the following primers: E1 mutant sense, 5'-GCCCTGGGTTTGATCTCCAGCAGAATTG GAAGAAAGG GATAGTAGGATAGATTG-3'; E2 mutant sense, 5'-TAAG GAAAATGTTCTACTAGTCC AGGTGCATGAAGTCGGGATCCACTTTGCC-3.

MITF deletion constructs were created by using Q5 site-directed mutagenesis kit (New England Biolabs, Inc.) on the original pCMV-MITF-H vector. The following primers were used: ceDel F GTCGACCTCGAGGATT AC; ceDel R TTGCTGTTCCCGTTGCAA; AD F TCAAGTATAATGAAGAAAT TTTGG; and AD R GTCATCAATTACATCATCCATC.

FHL2 deletion constructs were also created by site directed mutagenesis on the original FHL2-CMV5 vector, using combinations of the following forward primers: GGAAAGGATATTGTCGACG; GTGCCCTGCT ATGAGAAG; TCCAAGTGCCAGGAAT GC; TTGTACGCTAAGAAATGTG; and reverse primers: CAGGGCATACTGCTTCTC; GCAGTCAAAGCGTTCA GTC; CGAGTATTCATTGGAATAGC;

2.9. Transient co-transfection and luciferase assay

HEK293T cells were co-transfected using TransLT1 reagent (Mirus) with $0.25 \mu\text{g}$ of pCMV MITF-H or pcDNA-MITF wild type or *ce/ce* mutant MITF and $0.25 \mu\text{g}$ of wild type pGL3-Erbin or mutant reporter or the relevant empty reporter vector.

H9c2 cells were co-transfected using Jetprime reagent (Polyplus Transfection) with $0.25 \mu\text{g}$ of pCMV MITF-H and $0.25 \mu\text{g}$ Erbin pGL3 luciferase reporter. The cells were incubated in 24-well plates for 24 h. The cells were lysed and assayed for luciferase activity (Promega). The luciferase activity was normalized to the total protein concentration.

2.10. ChIP assay

The chromatin immunoprecipitation (ChIP) assay was performed as follows: NIH3T3 cells were transfected with the MITF-H isoform or FHL2 and were incubated with normal medium with or without $10 \mu\text{M}$ isoproterenol overnight. After 48 h the cells were treated with formaldehyde for protein-DNA cross-linking, chromatin extracted and then sonicated to give an average size of 300 to 1000 bp. Chromatin was incubated with anti-MITF or anti-FHL2 antibodies. Immunoprecipitation was performed overnight at 4°C with rotation. Samples were digested with proteinase K (Roche Applied Science). DNA was extracted by chloroform precipitation and resuspended in $20 \mu\text{l}$ of Tris (10mM)-EDTA (1mM) buffer. The DNA was used as a template for 30 cycles of PCR amplification with the following primers: E-box1 sense, 5'-CACTTATCCCT CGGGGTTT-3'; E-box1 antisense, 5'-CATCTTGGGGCTCAT TCTC-3'; E-box2 sense, 5'-AGGAATACAGGCGACAGACG-3'; E-box2 antisense, 5'-TTGTCCAAATAGGCAAAGTGG-3'; ubiquitin c, sense, 5'-CGTCGAGCCC AGTGTACC ACCAAGAAGG-3'; and antisense, 5'-CCCCATCACCCCAA GAACAAGCACAAAG-3'.

2.11. Yeast two-hybrid analysis

Protein interactions were assayed in yeast using a split-ubiquitin two-hybrid approach according to the manufacturer's protocol (Dualsystems Biotech). Bait and prey constructs were transformed into the yeast strain NMY32, plated on $-\text{Trp} - \text{Leu}$ selection plates, and incubated at 30°C for 3–4 days. Approximately five medium-size colonies were selected and resuspended in water. After all samples were diluted to equivalent densities, serial dilutions were spotted on selection plates $-\text{Trp} - \text{Leu}$, $-\text{Trp} - \text{Leu} - \text{His}$, and $-\text{Trp} - \text{Leu} - \text{His} + 10 \text{mM}$ 3-amino-1,2,4 triazole. After 3–4 days of growth at 30°C , the presence of protein interactions was determined using the most stringent selection.

2.12. In silico docking

FHL2 LIM domains 2, 3, and 4 (PDB code: 1X4K, 2D8Z, and 1X4L, respectively) were individually docked onto the MITF-DNA complex structure (PDB code: 4ATK) using the web based automatic protein docking server ZDOCK (<http://zdock.umassmed.edu>) [16]. All molecular surface exposed residues of MITF were unbiasedly used in the calculation. Top 10 ranked models were generated by the ZDOCK server, and

repetitive binding modes were then selected by superimposition of these models with MITF–DNA structure.

2.13. Statistics

Statistical analysis was performed by either 2-tailed Student's *t*-test or by two-way ANOVA with Tukey's HSD post-hoc test as appropriate. Null hypothesis was rejected at $p < 0.05$ level for all tests. Exact Mann–Whitney test was performed for all mice experiments. Wilcoxon rank sum test was performed on the luciferase data. For Figs. 1A and 3B–C, the combined *p* value was calculated by Fisher chi square test, data are reported as mean \pm SEM.

3. Results

3.1. Microarray analysis of hearts derived from MITF mutated mice

Since middle-aged MITF-mutated mice have a much smaller heart mass and have greatly decreased cardiac function and cardiac output [8], gene array analysis of RNA extracted from a pool of hearts from 15 month old MITF mutated mice (*ce/ce*) was carried out and compared to that of their wild type siblings (*sp/sp*) ($n = 5$). This analysis revealed more than 200 genes, the expression of which was significantly different between the two groups.

The data were compared to public gene arrays using Gene Expression Omnibus (GEO; <http://www.ncbi.nlm.nih.gov/geo/>) that shows changes in MITF expression in murine hearts in various conditions. The expression of only 25 genes was similarly changed in the compared gene array (Table S1). Erbin was chosen for further analysis since we have previously shown its involvement in cardiac hypertrophy [10].

Real-time quantitative PCR demonstrated increased Erbin mRNA levels in the hearts of 15 month old MITF-mutated mice compared to wild type littermates ($n = 7–9$, $p = 0.0265$; Fig. 1A). Increased

expression of Erbin in these MITF-mutated mice was further validated by Western blot analysis ($n = 4$; Fig. 1B).

3.2. Erbin expression is regulated by MITF

The mechanism by which MITF regulates Erbin expression was analyzed *in vitro* using H9c2 cells, a cardiomyoblast cell line derived from embryonic rat heart. Over-expression of MITF in H9c2 cells, increased Erbin protein level (Fig. 2A). In H9c2 cells transfected with an empty plasmid, isoproterenol treatment (Iso) induced upregulation of Erbin protein levels compared to untreated cells (Con) (Fig. 2B). However, in H9c2 cells over-expressing MITF, isoproterenol induced a significant decrease in Erbin expression compared to untreated MITF over-expressing cells (Fig. 2B), indicating that MITF inhibits Erbin expression during β -adrenergic stimulation in H9c2 cells.

As mentioned above, we have previously shown that MITF plays an essential role in β -adrenergic induced cardiac hypertrophy. MITF-mutated mice (*ce/ce*) have a diminished cardiac hypertrophic response to β -adrenergic stimulation, decreased cardiac function and a tendency for sudden death [8].

The effect of MITF on Erbin expression during cardiac hypertrophy was further studied in 6–8 week old *ce/ce* MITF-mutated mice and their normal littermates (*sp/sp*) by once daily administration of either saline or isoproterenol for 7 days. A significant reduction in Erbin mRNA level was observed in isoproterenol-treated normal littermates (Fig. 2C), but not in MITF-mutated mice ($n = 5$, $p = 0.015$). Erbin protein levels were decreased in hearts derived from normal mice treated with isoproterenol compared to saline control ($n = 4$; Fig. 2D), while isoproterenol induced Erbin expression in MITF-mutated mice ($n = 4$; Fig. 2D).

Thus, our results from both *in vitro* and *in vivo* models indicate that MITF increases Erbin expression under basal conditions, but inhibits Erbin expression during β -adrenergic induced cardiac hypertrophy.

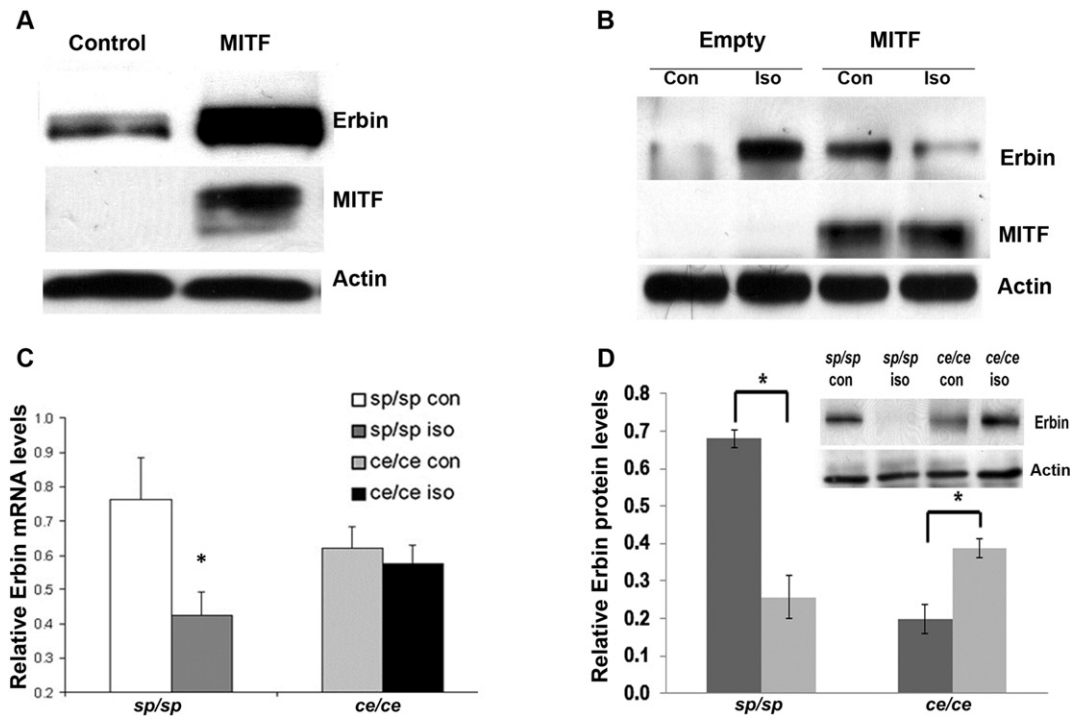


Fig. 2. Erbin expression is decreased in cardiac hypertrophy. A. H9c2 cells were transiently transfected with either MITF expression vector or with an empty plasmid used as control. 48 h after transfection the cells were lysed, and the levels of Erbin, MITF and β actin (control) were determined by Western blot analysis (one representative experiment out of two is shown). B. The effect of isoproterenol on Erbin expression. H9c2 cells were transiently transfected with either MITF or with an empty plasmid for 24 h, followed by overnight treatment with either saline (Con) or 10 μ M isoproterenol (Iso). Erbin protein levels were measured by Western blot analysis and normalized to β actin (one representative experiment out of three is shown). C. Real time PCR analysis of Erbin mRNA levels in *ce/ce* ($n = 5$) and *sp/sp* ($n = 5$) hearts. Mice were administered either saline (con) or isoproterenol (iso) once daily for 7 days. Results were normalized to β actin. Results represent mean \pm SEM. D. Western blot analysis of Erbin protein levels in hearts of *ce/ce* ($n = 4$) and their normal littermates (*sp/sp*) ($n = 4$). Mice were treated with either isoproterenol (iso) or saline (con). Bar graph represents the densitometry quantification of Western data, normalized to β actin. Results represent mean \pm SEM.

3.3. MITF regulates Erbin expression by binding two E-box elements

MITF binds CANNTG E-box elements in the promoters of its target genes [17]. Prediction of MITF binding sites in the Erbin promoter using MatInspector revealed two potential MITF E-box sites upstream to exon 1 at positions –2253 (E1) and –2809 (E2) (Fig. 3A). The Erbin promoter fragment containing these candidate E-box elements was cloned into a reporter vector and MITF transcriptional activity was measured. MITF over-expression significantly enhanced Erbin promoter activity both in H9c2 cells (n = 5; Fig. 3B) and in HEK293T cells (n = 7; combined, p = 0.00774) (Fig. 3C). HEK293T cells were transfected with a plasmid containing the truncated *ce/ce* MITF mutant

protein or wild type MITF. Transactivation of Erbin promoter by *ce/ce* MITF was greatly diminished compared to transactivation with wild type MITF (n = 3; Fig. 3C). H9c2 cells were co-transfected with Erbin promoter reporter and either the MITF expression vector or empty vector, and were incubated in serum-free medium with or without isoproterenol. The promoter activity decreased following isoproterenol administration in MITF over-expressing cells (n = 3; p = 0.05), while in empty vector cells no change was observed (Fig. 3D).

The Erbin promoter construct was point mutated at either the E1 or the E2 E-box element into aATtgG or CAGgTt, respectively. HEK293T cells were transiently co-transfected with either a mutant Erbin promoter or the wild type promoter, and with MITF expression vector.

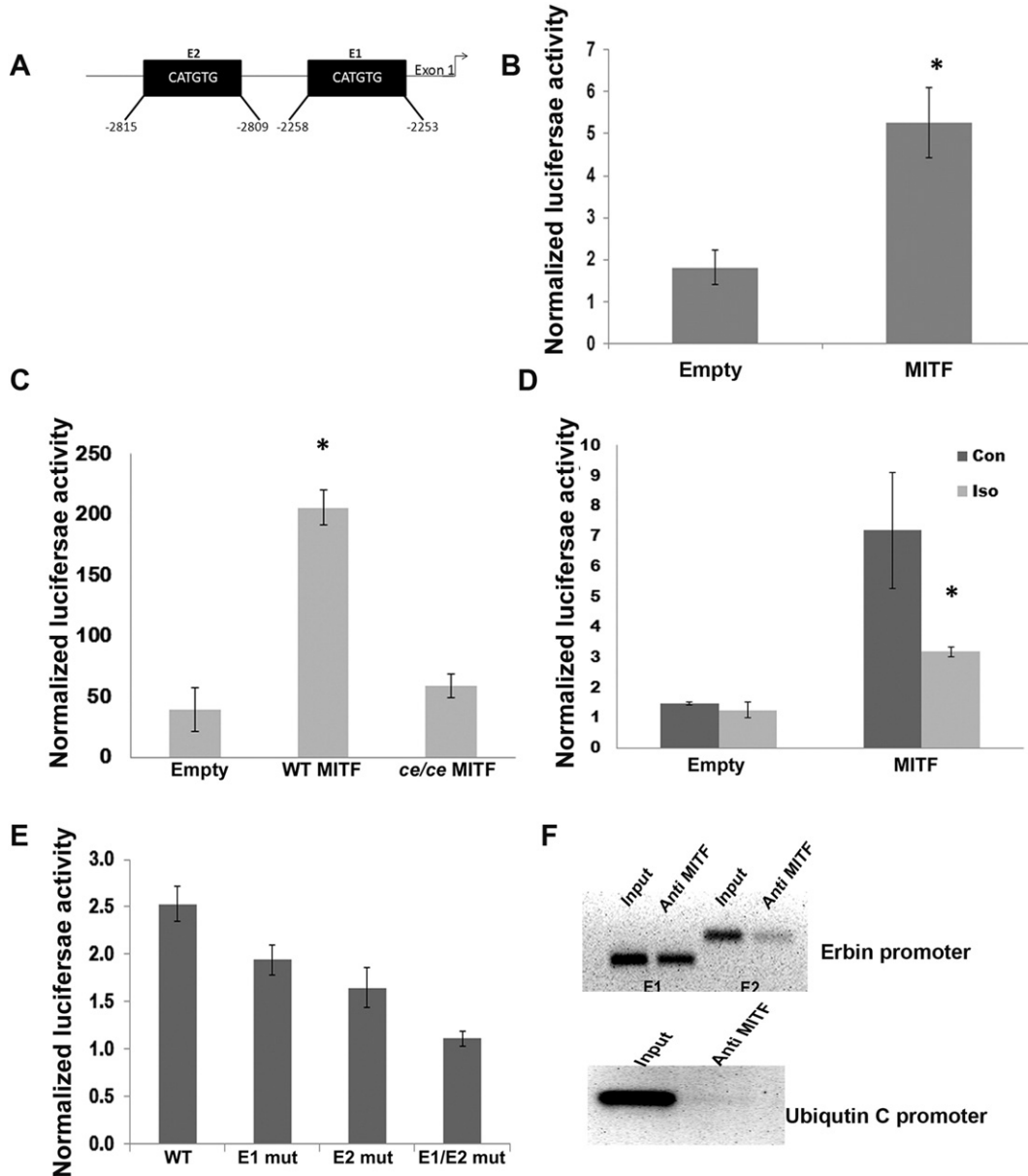


Fig. 3. MITF regulates Erbin expression. A. Schematic representation of the Erbin promoter containing two E-box elements (E1 and E2). B–C. WT MITF, *ce/ce* MITF or empty expression vector was co-transfected with the Erbin promoter reporter into H9c2 (n = 5) (B) and HEK293T cells (n = 7) (C) for 24 h. Luciferase activity was normalized to total protein levels. The results shown represent the mean ± standard deviation. D. Effect of isoproterenol on luciferase activity: either MITF expression vector or an empty vector was co-transfected with the Erbin promoter reporter into H9c2 cells for 24 h, followed by addition of 10 μM isoproterenol (Iso) or without addition (Con). Luciferase activity was normalized to total protein levels. Results represent mean ± SEM (n = 3). E. Wild type (WT), single mutants (E1 mut, E2 mut) or the double mutant (E1/E2 mut) of the Erbin promoter E-box elements was co-transfected with MITF expression vector or an empty vector into HEK293T cells. Luciferase activity was normalized against protein level and divided by the value obtained for the empty vector. The results shown represent the mean ± SEM (n = 5). F. Chromatin immunoprecipitation was performed on extracts of NIH3T3 cells overexpressing MITF. Immunoprecipitation was carried out using an anti-MITF antibody. Primers spanning the Erbin promoter at E1 and E2 E-box elements were used for PCR amplification. DNA before precipitation was used as control (input), whereas mouse ubiquitin C was used as a negative control (n = 3).

2.5-fold induction of Erbin promoter activity was observed in HEK293T cells over-expressing MITF compared to transfection with an empty vector. Interestingly, mutations in the E1 and E2 E-boxes resulted in a 30% and 50% decrease respectively in Erbin promoter activity compared to the wild type promoter (n = 5; Fig. 3E). Only the double mutation completely abolished the ability of MITF to transactivate the Erbin promoter, suggesting that both E boxes contribute to MITF's regulation of the Erbin promoter.

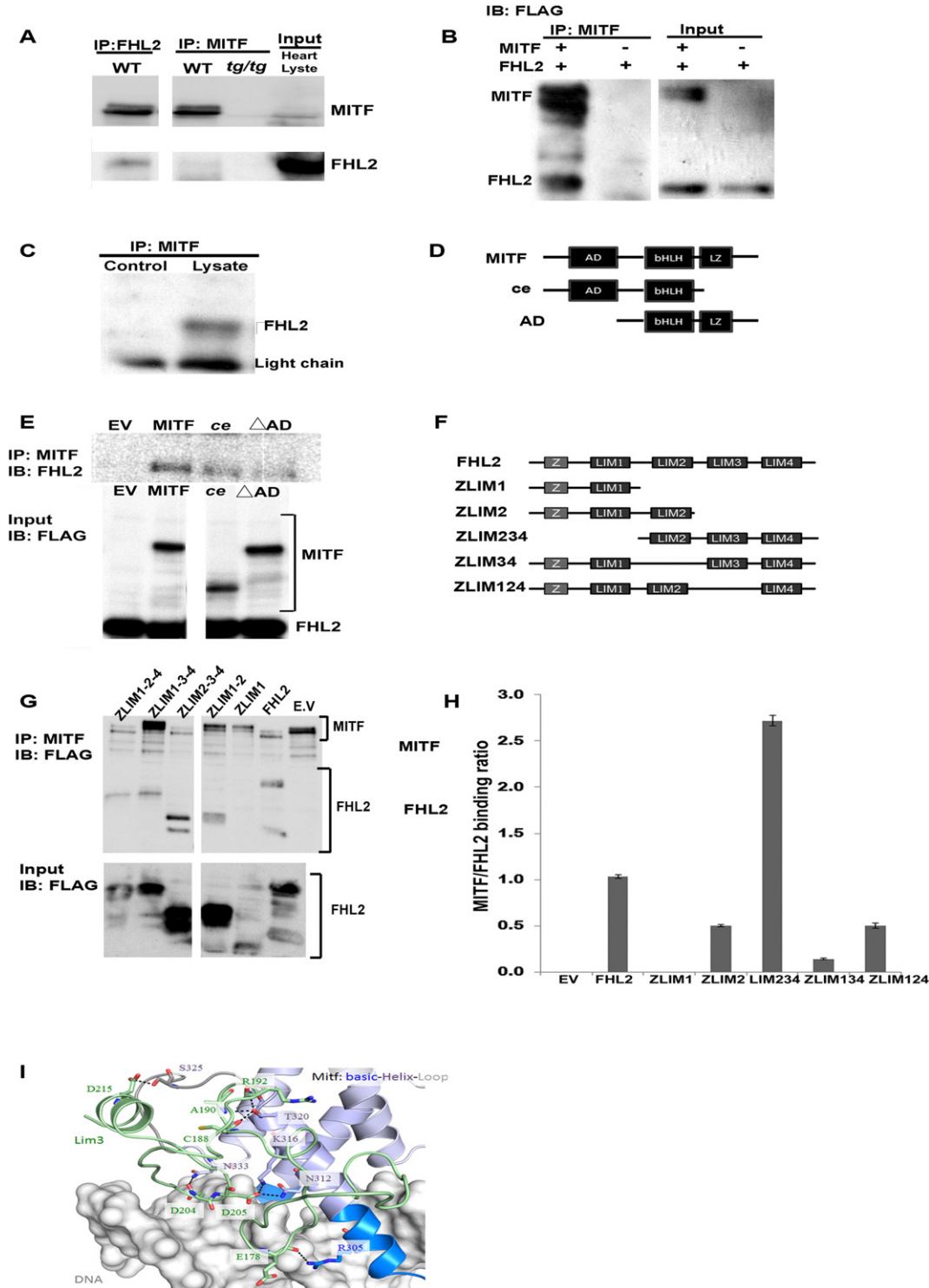
Further analysis of MITF binding to the Erbin promoter was performed using Chip assay. Chromatin complexes were immunoprecipitated with the anti-MITF antibody, and PCR was performed using primers to either

E-box elements (E1 and E2) or to ubiquitin C as a negative control. PCR amplification of the immunoprecipitate did not result in a ubiquitin C band, while a clear band was detected by specific amplification of the promoter regions containing both E-box elements (n = 3; Fig. 3F).

Thus, our results demonstrate that MITF regulates Erbin expression by binding both E-box elements of the Erbin promoter.

3.4. FHL2 interacts with MITF

Yeast two-hybrid screening was performed using a mouse heart library and full-length MITF heart isoform as a bait, in order to find



proteins that might be associated with MITF and that might mediate suppression of Erbin expression. FHL2 was found to be the protein most significantly associated with MITF in this assay. Co-immunoprecipitation of FHL2 and MITF was performed using heart lysates derived from either WT and *tg/tg* MITF deleted mice. MITF and FHL2 were found to associate using either anti-FHL2 or anti-MITF antibodies for immunoprecipitation (Fig. 4A). FHL2 co-immunoprecipitated with MITF only in HEK293T cells that were co-transfected with both FHL2 and MITF, but not in cells overexpressing only FHL2 (Fig. 4B). Endogenous MITF and FHL2 were found to be associated in a primary culture of neonatal rat cardiomyocytes (Fig. 4C). These results clearly indicate that FHL2 binds MITF in the heart.

The regions of MITF that mediated the interaction with FHL2 were mapped using MITF deletion constructs in a FLAG tagged vector (Fig. 4D). HEK293T cells were co-transfected with both FLAG-full length FHL2 expression vector and the various MITF deletion constructs, and co-immunoprecipitation with anti-MITF antibody was performed. Interaction was not hindered by the deletion of either the activation domain or the leucine zipper domain. These results indicate that the bHLH domain is required for the interaction with FHL2 (Fig. 4E).

FHL2 is a LIM domain binding protein. The LIM domain has been shown to be a potent protein–protein interaction motif [18]. Several FHL2 deletion constructs encoding different LIM domain combinations were generated to identify which LIM domain of FHL2 is responsible for the interaction with MITF (Fig. 4F). HEK293T cells were transiently transfected with full-length FLAG-MITF expression vector and either full-length FLAG-FHL2 expression vector or different FLAG-FHL2 LIM domain deletions. Co-immunoprecipitation was performed using anti-MITF antibody and immunoblotting was performed using anti-FLAG antibody (Fig. 4G, H). The zinc finger-LIM1 (ZLIM1) construct did not interact with MITF, however, interaction did occur when the LIM2 domain was added (ZLIM1-2). Furthermore, deletion of either LIM2 or LIM3 domain reduced interaction with MITF by 85% and 50%, respectively, compared to interaction with full length FHL2 (Fig. 4H). Therefore, both LIM2 and LIM3 domains participate in the interaction with MITF. Interestingly, truncation of the N terminal zinc finger and LIM1 (LIM2-3-4) increased the interaction with MITF 2.7-fold compared to full length FHL2.

The bHLH domain of MITF is the core region that interacts with the E-box DNA [19]. *In silico* docking of individual LIM2, 3, 4 domains of FHL2 to the bHLH domain–DNA complex indicates that only LIM2 and LIM3 domains show repetitive binding modes with the bHLH, and LIM3 domain gave the highest repetition (5 out of 10 top models showed the same binding mode) (Fig. 4I). The highest scored binding model shows that loops 161–166, 187–191, 202–205, and α -helix 210–217 regions of LIM3 interact with the “helix–loop” region of MITF. The predicted interactions include hydrogen bonds formed by residues: E178, C188, A190, R192, D204, D205, and D215 of FHL2, and the R305, N312, K316, T320, S325, and N333 of MITF (numbering as in human MITF-H).

3.5. FHL2 association with MITF mediates co-repression of Erbin expression

It has been reported that FHL2 can function as either a repressor or an activator of transcriptional activity [20,21]. In order to investigate if FHL2 affects MITF transcriptional activity, H9c2 cells were co-transfected with FHL2 and MITF expression vectors, and Erbin protein level was measured by Western blot analysis. Erbin level was reduced only by over-expression of both MITF and FHL2 (Fig. 5A). As previously shown, Erbin promoter activity was enhanced by MITF, while FHL2 expression alone had no effect. Simultaneous over-expression of both FHL2 and MITF significantly decreased Erbin promoter activity by about 50% ($n = 5$, $p = 0.0081$; Fig. 5B), thus indicating that FHL2 acts as an inhibitor of MITF transcriptional activity.

MITF–FHL2 association was further studied in 6–8 week old WT mice that received once daily administration of either saline or isoproterenol for 5 days. Isoproterenol's effect was validated by measuring heart weight to body weight ratio (Fig. S1). FHL2 mRNA levels were increased 2.2-fold in hearts from isoproterenol-treated wild type mice ($n = 6$, $p = 0.00216$; Fig. S2). This result is in accordance with a previous report [20]. In addition, co-immunoprecipitation of FHL2 and MITF (Fig. 5C–D) revealed that upon isoproterenol administration, FHL2 and MITF association increased 5-fold.

In order to determine whether FHL2 and MITF both bind Erbin promoter, chromatin immunoprecipitation was performed (Fig. 5E). MITF bound the Erbin promoter with or without isoproterenol. There was only faint binding of FHL2 in the absence of isoproterenol (lane 6). However, in the presence of isoproterenol, FHL2 binding to Erbin promoter was greatly enhanced (lane 4).

We recently reported that Erbin is downregulated in biopsies derived from human failing hearts [10]. Co-immunoprecipitation of FHL2 and MITF was performed using biopsies from either normal patients or heart failure patients (Fig. 5F). In human heart failure biopsies, FHL2 and MITF association was higher than in non-failing hearts.

These results suggest that FHL2 expression is induced by hypertrophic stimuli, and that FHL2 binds MITF and acts as a co-repressor of MITF, negatively regulating Erbin expression during cardiac hypertrophy.

4. Discussion

Cardiac hypertrophy followed by chronic heart failure (CHF) is a leading cause of death in Western nations. Recent improvements in cardiac revascularization therapy have reduced death due to myocardial infarction (MI), but there has been a steady increase in the number of individuals developing CHF after MI [22]. In stark contrast to the therapeutic developments in cardiac revascularization therapy, the molecular events leading from cardiac hypertrophy to CHF are still unclear, limiting the development of conceptually novel therapeutic approaches to the prevention of CHF.

We have previously described roles for both MITF and Erbin in cardiac hypertrophy and heart failure [8,10]. In the current work, we have

Fig. 4. MITF associates with FHL2. A. Co-immunoprecipitation of MITF and FHL2 in WT ($n = 4$) and *tg/tg* ($n = 2$) mice heart lysates using either anti-MITF or anti-FHL2 antibodies for immunoprecipitation (IP), with either anti-FHL2 or anti-MITF antibodies for immunoblotting (IB), respectively. The specificity of MITF band was verified using *tg/tg* MITF mice, which do not express MITF. B. HEK293T cells were co-transfected with FLAG-MITF and FLAG-FHL2 expression vectors or with FLAG-FHL2 and empty vector. Co-immunoprecipitation analysis demonstrated the binding of MITF and FHL2 using anti-MITF antibody for immunoprecipitation and anti-FLAG for immunoblotting (one experiment out of three is shown). C. Co-immunoprecipitation of FHL2 in primary neonatal rat cardiomyocytes (Lysate) using anti-MITF antibody for immunoprecipitation (IP) and anti-FHL2 antibody for immunoblotting. Mouse anti-MITF (Ab + beads) beads with lysis buffer was used as negative control (control) ($n = 3$) (one experiment out of two is shown). D. Schematic representation of MITF constructs used in the present study. AD, activation domain; B, basic; HLH, helix–loop–helix; LZ, leucine zipper. E. Co-immunoprecipitation of FHL2. HEK293T cells were co-transfected with FLAG-FHL2 expression vector and different MITF deletion constructs: MITF full length (MITF), MITF without LZ (ce) and MITF without the N terminal activation domain (AD). As control, HEK293T were transfected with equal concentration of empty vector. Co-immunoprecipitation analysis demonstrated the binding of MITF and FHL2 using anti-MITF antibody for immunoprecipitation and anti-FLAG for immunoblotting (one experiment out of three is shown). Input controls were analyzed by Western blotting, or immunoblotting (IB), using appropriate antibodies as indicated. F. Schematic representation of the FHL2–CMV5 deletion constructs. Zinc finger domain (Z); LIM domains (LIM1/LIM2/LIM3/LIM4). G. Co-immunoprecipitation of FHL2. HEK293T cells were co-transfected with FLAG-MITF expression vector and the following FHL2 deletion constructs: FHL2 full length (FHL2), zinc finger to LIM1 (ZLIM1), zinc finger to LIM2 (ZLIM1-2), without LIM2 (ZLIM1-3-4), without LIM3 (ZLIM1-2-4) and without ZLIM1 (LIM2-3-4). As control, HEK293T were transfected with equal concentration of empty vector. Co-immunoprecipitation analysis was performed using anti-MITF antibody for immunoprecipitation and anti-FLAG for immunoblotting (one experiment out of three is shown). H. Bar graph representing the densitometry quantification of the co-immunoprecipitation (G) using ImageLab 5.0 software (Biorad). Results are expressed as FHL2 levels that were normalized to MITF. I. FHL2 LIM3 domain (PDB: 2D8Z) was docked to MITF: basic–helix–loop–helix/DNA complex (PDB: 4ATK). LIM3 (green) and MITF are shown as cartoons. DNA is shown as white surface. The basic–helix–loop–helix regions of MITF are colored in marine, light blue, gray, and light blue, respectively. The potential interacting residues are shown as sticks. The numbering of MITF residues is based on MITF-H (UniProtKB: O75030-7). Hydrogen bonds are indicated with dashes.

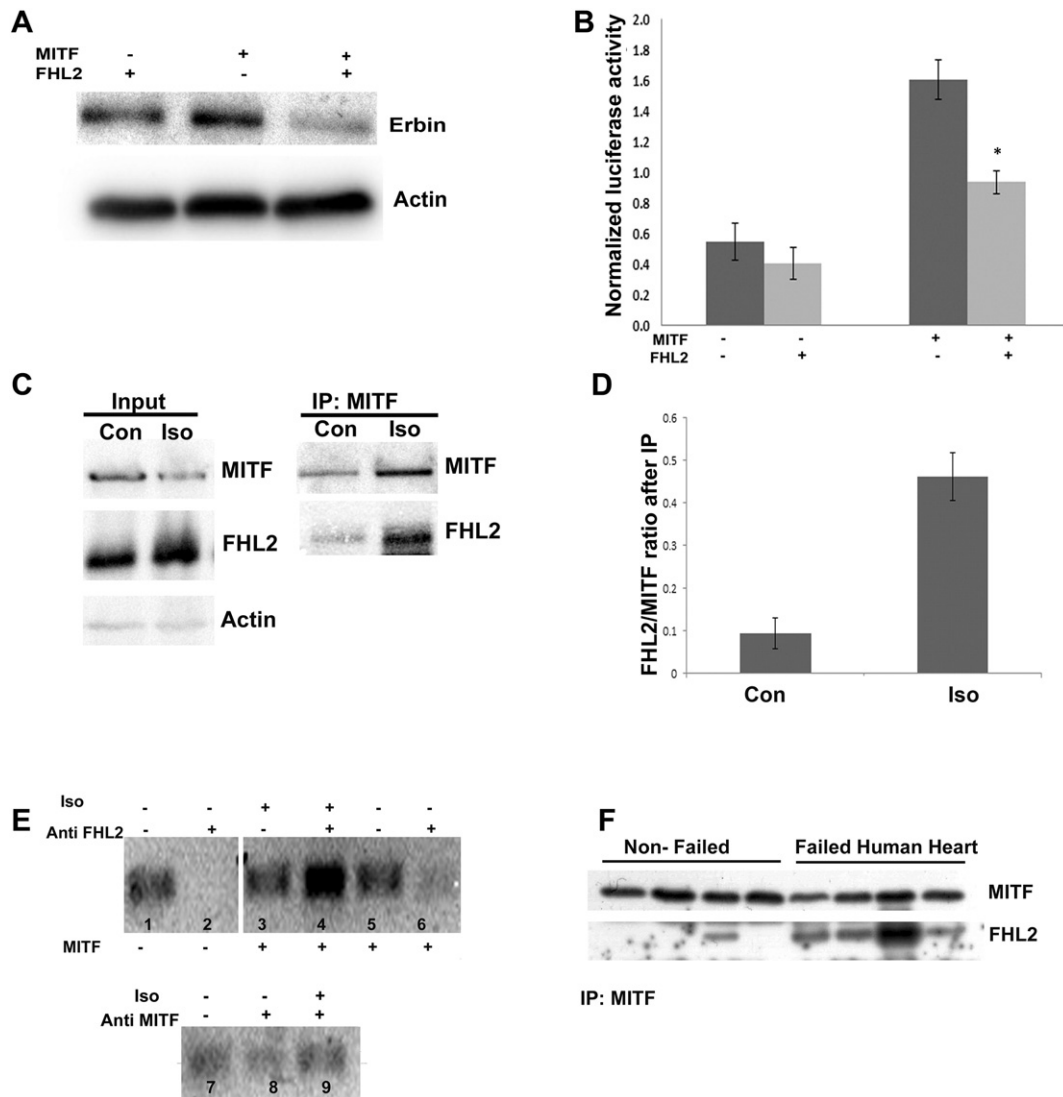


Fig. 5. FHL2 associates with MITF, mediating repression of Erbin expression. **A.** H9c2 cells were transiently transfected with either MITF or FHL2 expression vectors, or co-transfected with both expression vectors. 48 h after transfection cells were lysed and the level of Erbin was determined by Western blot analysis and compared to β -actin levels (one representative experiment out of three is shown). **B.** NIH3T3 cells were transiently transfected with either MITF or FHL2 expression vectors or co-transfected with both expression vectors, together with Erbin promoter reporter. After 24 h, luciferase activity was measured and normalized to protein levels. Results represent mean \pm SEM ($n = 5$). **C.** Co-immunoprecipitation of MITF and FHL2. Mice were injected with either isoproterenol (iso) ($n = 6$) or saline (con) ($n = 5$). Heart lysates were co-immunoprecipitated with anti-MITF antibody and immunoblotted with anti-FHL2 and anti-MITF antibodies. Input controls were analyzed by Western blotting, using anti-MITF, anti-FHL2 and anti- β actin antibodies. **D.** Bar graph representing the densitometry quantification of the co-immunoprecipitation (**C**) using ImageLab 5.0 software (Biorad), results are expressed as FHL2 levels that were normalized to MITF. **E.** Chromatin immunoprecipitation of MITF and FHL2 with Erbin promoter. Chromatin immunoprecipitation was performed on extracts of NIH3T3 cells over-expressing either MITF and FHL2 (lane 3–9) or FHL2 alone (lane 1–2). Immunoprecipitation was carried out using anti-FHL2 (top) or anti-MITF antibodies (bottom). Primers spanning the Erbin promoter were used for PCR amplification. Input DNA was used as a positive control (lanes 1, 3, 5, 7). Isoproterenol (Iso) was added to the medium for 24 h (lanes 3, 4, 9). **F.** Co-immunoprecipitation of MITF and FHL2 in human hearts. Extracts from human heart biopsies from normal patients (failed human hearts; $n = 9$) were immunoprecipitated with anti-MITF antibody. Western blot analysis with anti-MITF and anti-FHL2 antibodies was performed. One representative experiment with 4 samples for each group is shown.

demonstrated opposing functions of MITF, which activates Erbin expression in the basal state, but represses Erbin expression during cardiac hypertrophy.

We found that under basal conditions, MITF transactivates Erbin expression by binding two E-box elements in the Erbin promoter, a mechanism that has been described often in the literature. In contrast, suppression of target gene expression by MITF has seldom been reported. It is known, however, that while MITF collaborates with PU.1 transcription factor to transactivate osteoclast target genes such as cathepsin K and acid phosphatase during osteoclast differentiation [23], it can repress transcription of these same target genes in committed myeloid precursors capable of forming either macrophages or osteoclasts. This repression is mediated through direct interaction with the zinc finger protein Eos, an Ikaros family member, and enrichment of

known histone modifiers, such as histone deacetylase 1 (HDAC1) and sin3 transcription regulator family member A (Sin3A) bound to target genes. MITF acts as a modifier of chronic kidney diseases progression. MITF interacts with histone deacetylase 1 in cortical thick ascending limb cells, to repress the transcription of TGF- α , and antagonizes transactivation by its related partner, transcription factor E3 (TFE3) [24].

We therefore conducted a yeast two-hybrid screen in order to search for a previously unknown cardiac transcription inhibitor. We found that MITF associates with FHL2, a protein belonging to the LIM family that was found to be abundant and preferentially expressed in the heart [18]. The LIM domain coordinates two zinc ions, and establishes a tandem zinc-finger topology with a two-residue spacer between these zinc-finger modules [25].

FHL2^{-/-} mice have normal hearts under basal conditions, but have an exaggerated response to β-adrenergic stimulation [26], and FHL2 can suppress pathological cardiac hypertrophy [27]. FHL2 association with Nur77 prevents it from binding to enolase 3 promoter, and inhibits its transcription [28]. FHL2 was also shown to associate with promyelocytic leukemia zinc finger protein (PLZF), a known sequence-specific DNA-binding transcriptional repressor, and was able, *in vitro*, to further down-regulate target genes [29]. Previous yeast two-hybrid data suggest FHL2 association with both winged-helix/forkhead protein myocyte nuclear factor (MNF) [26,29] and with nuclear receptor corepressor 1 (NcoR1) [29], suggesting that FHL2 can be a co-repressor, but these data have never been substantiated.

Here we have shown that isoproterenol induces FHL2 expression; this result is in accordance with the previously described induction of FHL2 by isoproterenol [20]. Furthermore, isoproterenol also induces MITF-FHL2 association and Erbin promoter binding by both MITF and FHL2, resulting in down-regulation of Erbin expression. FHL2 alone, however, cannot bind Erbin promoter or repress its expression, and the presence of MITF is necessary for both. These data suggest that FHL2 functions as a co-repressor of Erbin expression.

Over the last few years it has become clearer that co-repression is not an “all-or-nothing” phenomenon, but can fine-tune expression of

active genes, and keep genes poised on the verge of transcription, giving precise control over the expression level of target genes, potentially with different consequences for each level [see review 30]. Repression seems to play an important role in development, determination of cell fate, and in disease [30,31]. Indeed, repression has an important role in cardiac hypertrophy [32].

Our results indicate that LIM2 and LIM3 domains in FHL2 and the bHLH domain in MITF are critical for MITF-FHL2 interaction. Docking prediction suggests that the interaction with MITF occurs at the basic-helix region of the HLH. Interestingly, full length FHL2 interaction with MITF is weaker than partial constructs that do not contain the zinc finger domain and LIM1. From the surfaces of the four FHL2 domains, it appears that Zinc-LIM1 is negatively charged, while LIM3 is positively charged, suggesting domain-domain contacts inside the FHL2 protein. No full length FHL2 structure is available, and FHL2 protein may assume a 4-D folding that is less favorable for MITF binding (Fig. 6).

We attempted to create a double Erbin-MITF knockout mouse strain in order to substantiate the critical importance of the proposed Erbin-MITF pathway in cardiac hypertrophy. However, despite prolonged efforts, we have not been able to obtain even one double knockout mouse. While each component is not essential to normal physiological functioning since there are compensatory mechanisms and neither

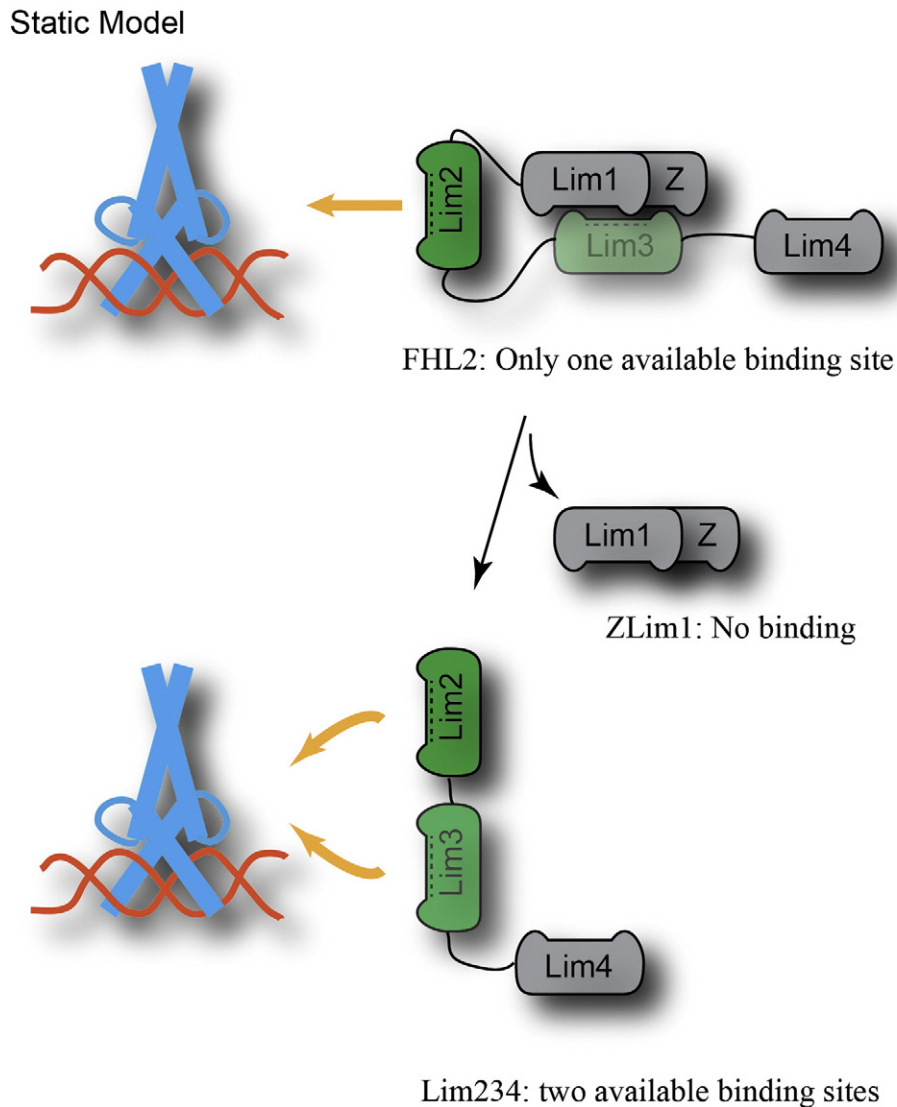


Fig. 6. FHL2-MITF binding model. FHL2-MITF static binding model based on co-immunoprecipitation of MITF and FHL2 deletion constructs. MITF is represented in blue, DNA in orange and FHL2 domains are represented in green and gray.

MITF nor Erbin knockout mice have a significant cardiac phenotype under normal conditions, presumably compensation is not possible when both components are lacking.

At present, we do not know if FHL2 is able to co-repress other MITF target genes or if it is able to associate and co-repress other MiT family members. Recently, FHL2 has been implicated in several physiological and pathological processes, including the proliferation and invasive growth of human MCF-7 breast cancer cells, aggravation of liver fibrosis in mice, mesenchymal cell osteogenic differentiation and bone formation. All of these conditions may potentially be mediated through interaction with MiT family members, and further exploration of FHL2-MiT interactions is warranted.

Conflict of interest

The authors declare no conflict of interest.

Acknowledgments

We would like to thank L. Lamoreux (College of Veterinary Medicine, Texas A&M University, and College Station, Texas, USA) for *sp/sp* and MITF *sp/ce* mice; H. Arnheiter (NIH, Bethesda, Maryland, USA) for *VGA-9^{fl/+}* mice; Prof. Jean Borg (Institut National de la Santé et de la Recherche Médicale, Marseille, France) for the anti-Erbin antibody; Rachel Hashuel for the help in the experiments; and Prof. Paul Riley (Oxford University) for FHL2-CMV5 vector. We would like to thank Prof Norman Grover from The Hebrew University for the statistical analysis.

This research was supported by the Israel Science Foundation [1925/12 to S.T and 115/2013 to E.R.], the United States Binational Science Foundation [2007220 to E.R. and D.E.F.]; the National Research Foundation of Singapore [HUI-CREATE to E.R.], by the NIH [R01 AR043369-18 and P01 CA163222 to D.E.F.], and by a grant from the Dr. Miriam and Sheldon G. Adelson Medical Research Foundation [to D.E.F.].

Appendix A. Supplementary data

Supplementary data to this article can be found online at <http://dx.doi.org/10.1016/j.ijcard.2015.05.108>.

References

- [1] C.A. Hodgkinson, K.J. Moore, A. Nakayama, E. Steingrimsson, N.G. Copeland, N.A. Jenkins, et al., Mutations at the mouse microphthalmia locus are associated with defects in a gene encoding a novel basic-helix-loop-helix-zipper protein, *Cell* 74 (1993) 395–404.
- [2] M.J. Hughes, J.B. L., J.M. Krakowsky, K.P. Anderson, A helix-loop-helix transcription factor-like gene is located at the mi locus, *J. Biol. Chem.* 268 (1993) 20687–20690.
- [3] K.J. Moore, Insight into the microphthalmia gene, *Trends Genet.* 11 (1995) 442–448.
- [4] M. Tassabehji, V.E. Newton, A.P. Read, Waardenburg syndrome type 2 caused by mutations in the human microphthalmia (MITF) gene, *Nat. Genet.* 8 (1994) 251–255.
- [5] T.J. Hemesath, E. Steingrimsson, G. McGill, M.J. Hansen, J. Vaught, C.A. Hodgkinson, et al., Microphthalmia, a critical factor in melanocyte development, defines a discrete transcription factor family, *Genes Dev.* 8 (1994) 2770–2780.
- [6] H. Nechushtan, Z. Zhang, E. Razin, Microphthalmia (mi) in murine mast cells: regulation of its stimuli-mediated expression on the translational level, *Blood* 89 (1997) 2999–3008.
- [7] S. Tshori, A. Sonnenblick, N. Yannay-Cohen, G. Kay, H. Nechushtan, E. Razin, Microphthalmia transcription factor isoforms in mast cells and the heart, *Mol. Cell. Biol.* 27 (2007) 3911–3919.
- [8] S. Tshori, D. Gilon, R. Beeri, H. Nechushtan, D. Kaluzhny, E. Pikarsky, et al., Transcription factor MITF regulates cardiac growth and hypertrophy, *J. Clin. Invest.* 116 (2006) 2673–2681.
- [9] J.P. Borg, S. Marchetto, A. Le Bivic, V. Ollendorff, F. Jaulin-Bastard, H. Saito, et al., ERBIN: a basolateral PDZ protein that interacts with the mammalian ERBB2/HER2 receptor, *Nat. Cell Biol.* 2 (2000) 407–414.
- [10] I. Rachmin, S. Tshori, Y. Smith, A. Oppenheim, S. Marchetto, G. Kay, et al., Erbin is a negative modulator of cardiac hypertrophy, *Proc. Natl. Acad. Sci. U. S. A.* 111 (2014) 5902–5907.
- [11] D. Liu, M. Shi, H. Zhang, L. Qian, M. Yu, M. Hu, c-Myb Regulates Cell Cycle-Dependent Expression of Erbin: An Implication for a Novel Function of Erbin, *PLoS One* (2014) 7: e42903.
- [12] P.H. Chu, P. Ruiz-Lozano, Q. Zhou, C. Cai, J. Chen, Expression patterns of FHL/SLIM family members suggest important functional roles in skeletal muscle and cardiovascular system, *Mech. Dev.* 95 (2000) 259–265.
- [13] H. Hallaq, Y. Hasin, R. Fixler, Y. Eilam, Effect of ouabain on the concentration of free cytosolic Ca⁺⁺ and on contractility in cultured rat cardiac myocytes, *J. Pharmacol. Exp. Ther.* 248 (1989) 716–721.
- [14] M. Movassagh, M.K. Choy, M. Goddard, M.R. Bennett, T.A. Down, R.S. Foo, Differential DNA methylation correlates with differential expression of angiogenic factors in human heart failure, *PLoS One* 5 (2010) e8564.
- [15] E. Steingrimsson, K.J. Moore, M.L. Lamoreux, A.R. Ferre-D'Amare, S.K. Burley, D.C. Zimring, et al., Molecular basis of mouse microphthalmia (mi) mutations helps explain their developmental and phenotypic consequences, *Nat. Genet.* 8 (1994) 256–263.
- [16] B.G. Pierce, K. Wiehe, H. Hwang, B.H. Kim, T. Vreven, Z. Weng, ZDOCK server: interactive docking prediction of protein-protein complexes and symmetric multimers, *Bioinformatics* 30 (2014) 1771–1773.
- [17] E. Morii, T. Tsujimura, T. Jippo, K. Hashimoto, K. Takebayashi, K. Tsujino, et al., Regulation of mouse mast cell protease 6 gene expression by transcription factor encoded by the mi locus, *Blood* 88 (1996) 2488–2494.
- [18] K.K. Chan, S.K. Tsui, S.M. Lee, S.C. Luk, C.C. Liew, K.P. Fung, et al., Molecular cloning and characterization of FHL2, a novel LIM domain protein preferentially expressed in human heart, *Gene* 210 (1998) 345–350.
- [19] V. Pogenberg, M.H. Ogmundsdottir, K. Bergsteinsdottir, A. Schepsky, B. Phung, V. Deineko, et al., Restricted leucine zipper dimerization and specificity of DNA recognition of the melanocyte master regulator MITF, *Genes Dev.* 26 (2012) 2647–2658.
- [20] B. Hojavey, B.A. Rothermel, T.G. Gillette, J.A. Hill, FHL2 binds calcineurin and represses pathological cardiac growth, *Mol. Cell. Biol.* 32 (2012) 4025–4034.
- [21] R. Matsunaga-Udagawa, Y. Fujita, S. Yoshiki, K. Terai, Y. Kamioka, E. Kiyokawa, et al., The scaffold protein Shoc2/SUR-8 accelerates the interaction of Ras and Raf, *J. Biol. Chem.* 285 (2010) 7818–7826.
- [22] R. Kumarswamy, T. Thum, Non-coding RNAs in cardiac remodeling and heart failure, *Circ. Res.* 113 (2013) 676–689.
- [23] R. Hu, S.M. Sharma, A. Bronisz, R. Srinivasan, U. Sankar, M.C. Ostrowski, Eos, MITF, and PU.1 recruit corepressors to osteoclast-specific genes in committed myeloid progenitors, *Mol. Cell. Biol.* 27 (2007) 4018–4027.
- [24] D. Laouari, M. Burtin, A. Phelep, F. Bienaime, L.H. Noel, D.C. Lee, et al., A transcriptional network underlies susceptibility to kidney disease progression, *EMBO Mol. Med.* 4 (2012) 825–839.
- [25] J.L. Kadmas, M.C. Beckerle, The LIM domain: from the cytoskeleton to the nucleus, *Nat. Rev. Mol. Cell Biol.* 5 (2004) 920–931.
- [26] Y. Kong, J.M. Shelton, B. Rothermel, X. Li, J.A. Richardson, R. Bassel-Duby, et al., Cardiac-specific LIM protein FHL2 modifies the hypertrophic response to beta-adrenergic stimulation, *Circulation* 103 (2001) 2731–2738.
- [27] R. Okamoto, Y. Li, K. Noma, Y. Hiroi, P.Y. Liu, M. Taniguchi, et al., FHL2 prevents cardiac hypertrophy in mice with cardiac-specific deletion of ROCK2, *FASEB J.* 27 (2013) 1439–1449.
- [28] K. Kurakula, E. van der Wal, D. Geerts, C.M. van Tiel, C.J. de Vries, FHL2 protein is a novel co-repressor of nuclear receptor Nur77, *J. Biol. Chem.* 286 (2011) 44336–44343.
- [29] P. McLoughlin, E. Ehler, G. Carlile, J.D. Licht, B.W. Schafer, The LIM-only protein DRAL/FHL2 interacts with and is a corepressor for the promyelocytic leukemia zinc finger protein, *J. Biol. Chem.* 277 (2002) 37045–37053.
- [30] N. Reynolds, A. O'Shaughnessy, B. Hendrich, Transcriptional repressors: multifaceted regulators of gene expression, *Development* 140 (2013) 505–512.
- [31] V. Perissi, K. Jepsen, C.K. Glass, M.G. Rosenfeld, Deconstructing repression: evolving models of co-repressor action, *Nat. Rev. Genet.* 11 (2010) 109–123.
- [32] P. Mathiyalagan, S.T. Keating, X.J. Du, A. El-Osta, Chromatin modifications remodel cardiac gene expression, *Cardiovasc. Res.* 103 (2014) 7–16.